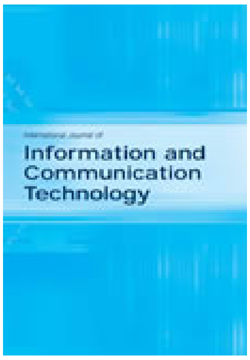

International Journal of Information and Communication Technology

ISSN online: 1741-8070 - ISSN print: 1466-6642
https://www.inderscience.com/ijict

Dynamic performance of a delayed-onset disease model including death and recovery

Quanhao Song

Article History:

Received:	24 September 2024
Last revised:	30 October 2024
Accepted:	30 October 2024
Published online:	13 December 2024

Dynamic performance of a delayed-onset disease model including death and recovery

Quanhao Song

School of Sciences,
Southwest Petroleum University,
Chengdu, Sichuan, 610500, China
Email: jysqhccc666@126.com

Abstract: Due to the complex and constantly evolving process of infectious disease transmission, we have studied a class of delayed SIR models incorporating both death and recovery to control the spread of diseases. We creatively use bifurcation theories to determine the critical delay τ_0 for Hopf bifurcation to comprehend the impact of time delay on the system. The analysis of periodic solutions and bifurcation directions, based on central manifold and normal form theory, offers insights into the system's dynamics. Simulations utilising time series charts and trajectory diagrams aid in comprehending the impact of hysteresis parameters. Additionally, data fitting is performed to verify the proposed model by contrasting it with actual data. The research demonstrates that the implementation of consistent preventive and hygienic measures can significantly reduce the severity of disease exacerbation.

Keywords: SIR model; basic reproductive number; time delay; Hopf bifurcation; centre manifold theorem.

Reference to this paper should be made as follows: Song, Q. (2024) 'Dynamic performance of a delayed-onset disease model including death and recovery', *Int. J. Information and Communication Technology*, Vol. 25, No. 10, pp.1–18.

Biographical notes: Quanhao Song is a Master's student at Southwest Petroleum University. His research directions are infectious disease prevention and control, differential equations and dynamical systems, and machine learning.

1 Introduction

Infectious diseases have long been among the most serious health challenges faced by human society, with their impacts not confined to the medical field but also extending into multiple aspects, including the economy, society, and politics. From the Black Death (DeWitte, 2018) to Ebola virus (Malik et al., 2023), from tuberculosis (Paton et al., 2023) to HIV (Lestari, 2016), various infectious diseases continue to threaten human health and life safety. The spread of infectious disease constitute a intricate and constantly evolving process, influenced by various factors including social network (Yin et al., 2024), population structure (Moreira et al., 2010), environmental (Maier et al., 2021), and behavioural habits (Damgacioglu et al., 2023).

By combining complex socio-economic data with multi-dimensional vector coordinates, Leowski (2010) realised the efficient organisation, management and analysis of data, and offered robust support for the prevention efforts aimed at infectious diseases. In response to new threats, it is essential to comprehend and anticipate the dissemination patterns of diseases. This not only helps to implement effective prevention and control measures but also guides the formulation of public health policies and responses to sudden infectious disease outbreaks. The dynamics of infectious diseases have emerged as a critical area of study. Many scientists have established various mathematical models to analyse their dynamic behaviour.

The prevention and control of infectious diseases also require real-time monitoring of epidemic data, population flow information, and the dynamics of public health events (Cui et al., 2022). Their method, which is based on a sequence logic model, can be used to design an efficient monitoring system capable of capturing the early signs of an epidemic.

The seminal SIR model was introduced by Kermack and McKendrick (1927), which can forecast the development trend of the epidemic and provide an important reference for public health policy-making. Subsequently, many scientists also extended SIR model and proposed models such as SEIRS (Shao and Shateyi, 2021), SEIR (Shoaib et al., 2023), SIRS (Li et al., 2017), SEIS (Yang, 2016), and SIS (Meng et al., 2016).

Time delay refers to the lag effect of certain processes, which often occurs in the real-world dissemination of diseases. For example, the onset of symptoms after infection requires a certain incubation period, and treatment also requires a certain recovery time. Therefore, considering the time delay factor in infectious disease models is crucial for more accurately describing the dynamic process of infectious disease transmission. Barman and Mishra (2023) took into account the SIR model with time delays and a nonlinear incidence rate, and introduced population mobility through a graph network. Mvogo et al. (2023) analysed the SIRS model while considering both diffusion and delay factors, ultimately revealing that the delay term is directly proportional to the diffusion rate.

Time delay factors have a significant impact on the spread of infectious diseases. For example, time delays may lead to system instability, the emergence of periodic solutions, and bifurcation phenomena. Zhao et al. (2014) introduced an SIRS model that integrates media coverage and incorporates a time delay factor, as follows:

$$\begin{cases} \dfrac{dS}{dt} = b - dS - \left(\beta_1 - \dfrac{\beta_2}{e+I}\right) IS + \gamma R, \\ \dfrac{dI}{dt} = \left(\beta_1 - \dfrac{\beta_2}{e+I}\right) IS - (c+\theta)I, \\ \dfrac{dR}{dt} = \mu I - (e+\xi)R. \end{cases}$$

Then they delve into the local asymptotic stability of the equilibria and subsequently discuss the conditions under which periodic orbits undergo bifurcation. Furthermore, they demonstrate that the occurrence of a local Hopf bifurcation implies the emergence of a global Hopf bifurcation following the second critical delay value.

Zhen et al. (2006) introduced an SIRS model that considers the dissemination of the disease via vectors, which require an incubation period before becoming infectious. Furthermore, it is established that the endemic equilibrium point exhibits global stability in the context of a 'weak delay'.

Inspired by previous research, Tchuenche and Nwagwo (2009) proposed a class of time-delay SIR models. They used the Lyapunov function method for stability analysis, ascertained the maximum number of critical delays that give significance and validity to the model, and finally verified the conclusion through numerical simulation. Model details:

$$\begin{cases} \dfrac{dS}{dt} = -\beta I(t-\tau)Se^{-\mu_1\tau} - \mu S + \gamma \\ \dfrac{dI}{dt} = I(t-\tau)S\beta e^{-\mu_1\tau} - (\xi + \mu)I \\ \dfrac{dR}{dt} = \xi I - \mu R \end{cases} \quad (1)$$

The parameters are explained in Table 1.

Table 1 The biological significance of each parameter of system (1)

β	The effective rate of daily contact between people
τ	The time lag
μ_1	Case fatality rate in the range of $(0, \tau)$
μ	Natural mortality rate of population
γ	Birth rate of people
ξ	Recovery rate of infected patients

Changes in time delay cause the equilibrium point of the model to undergo Hopf bifurcation, resulting in a periodic bifurcation solution. These cyclic solutions pose challenges for the prevention and control of infectious diseases and require a deeper understanding of their dynamics. However, previous researchers have focused solely on analysing the stability of the equilibrium point, neglecting a detailed examination of the Hopf bifurcation. Consequently, there is an incomplete understanding of the impact of time delay on the system, a lack of ability to predict the complex dynamic behaviour of disease transmission, and potentially missed opportunities for control. In this situation, we creatively incorporated the study of Hopf bifurcation into the analysis of delayed infectious diseases, and used the central manifold theorem and normal form theory to analyse bifurcation directions and periodic solutions, providing a new perspective for understanding complex dynamic systems and infectious disease prevention and control.

The organisation of this article is as outlined below. Initially, we conduct a thorough analysis of the Hopf bifurcation near the endemic equilibrium point, building upon the previously established model. Subsequently, we meticulously examine the direction of the bifurcation and the stability of the resulting periodic solutions. Finally, we validate our findings and theorems through rigorous numerical simulations, ensuring the robustness and applicability of our results.

2 Dynamics analysis

2.1 The previous result

Drawing upon the cumulative achievements of numerous scholars, Tchuenche and Nwagwo proposed an innovative time-delay SIR model:

$$\begin{cases} \dfrac{dS}{dt} = -SI(t-\tau)\beta e^{-\mu_1\tau} - \mu S + \gamma \\ \dfrac{dI}{dt} = \beta S e^{-\mu_1\tau} I(t-\tau) - (\xi+\mu)I \\ \dfrac{dR}{dt} = \xi I - \mu R \end{cases}$$

Tchuenche and Nwagwo have previously established the boundedness of the solution and employed the Lyapunov second method to demonstrate the local asymptotic stability of two equilibrium points.

Since the first two equations are independent of the second equation, we simplify the above equation system to obtain:

$$\begin{cases} \dfrac{dS}{dt} = -SI(t-\tau)\beta e^{-\mu_1\tau} - \mu S + \gamma \\ \dfrac{dI}{dt} = S\beta I(t-\tau) e^{-\mu_1\tau} - (\mu+\xi)I \end{cases} \tag{2}$$

2.2 Bifurcation analysis

2.2.1 Analysis steps

In order to clearly illustrate the mathematical derivation process of bifurcation analysis, we have created Figure 1.

Figure 1 The flowchart of bifurcation analysis

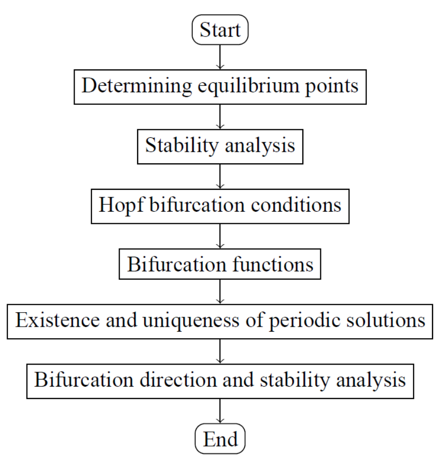

2.2.2 *Hopf bifurcation*

Considering its biological significance, the initial condition of the model is $\phi = \{\phi_1, \phi_2\}, \mathbf{C}_+ = \{\phi \in \mathbf{C}([-\tau, 0]), \mathbf{R}_+^2\}$, where $\mathbf{R}_+^2$ is two dimensional positive vector space.

In the previous paper (Tchuenche and Nwagwo, 2009), they compute $\mathcal{R}_0$ by utilising the regeneration matrix theorem.

$$\mathcal{R}_0 = \frac{\beta e^{-\mu_1 \tau}}{\mu + \xi}$$

To find the equilibrium of the model, we set all derivatives to zero in system (2), and solve the system as follows:

$$\begin{cases} -\beta S_* e^{-\mu_1 \tau} I_* + \gamma - \mu S_* = 0 \\ S_* I_* \beta e^{-\mu_1 \tau} - (\xi + \mu) I_* = 0 \end{cases}$$

such that

$$S_* = \frac{\mu + \xi}{\beta} e^{\mu_1 \tau}, I_* = \frac{\gamma}{\mu + \xi} - \frac{\mu}{\beta} e^{\mu_1 \tau}.$$

Therefore, according to the above calculation, $E_* = (\frac{\mu+\xi}{\beta} e^{\mu_1 \tau}, \frac{\gamma}{\mu+\xi} - \frac{\mu}{\beta} e^{\mu_1 \tau})$ is acquired by us.

Calculate the characteristic equation of model at E_*:

$$\begin{vmatrix} \lambda + \mu + \beta e^{-(\mu_1+\lambda)\tau} I_* & \beta e^{-(\mu_1+\lambda)\tau} S_* \\ -\beta e^{-(\mu_1+\lambda)\tau} I_* & \lambda + \mu + \xi - \beta e^{-(\mu_1+\lambda)\tau} S_* \end{vmatrix} = 0$$

obtain:

$$\lambda^2 + m_1 \lambda + m_2 + e^{-(\mu_1+\lambda)\tau} (m_3 \lambda + m_4) = 0 \tag{3}$$

where

$$m_1 = 2\mu + \xi, m_2 = \mu^2 + \mu\xi, m_3 = \beta I_* - \beta S_*, m_4 = \beta I_* \mu - \beta S_* \mu + \beta I_* \xi.$$

Suppose $\lambda = i\omega$ is a pure imaginary root in equation (3), substitute into the original equation:

$$-\omega^2 + i m_1 \omega + m_2 + (\cos(\tau\omega) - i \sin(\omega\tau)) e^{-\mu_1 \tau} (i m_3 \omega + m_4) = 0$$

Separate the real and imaginary parts, we acquire,

$$\begin{cases} m_4 \cos(\tau\omega) + m_3 \omega_1 \sin(\tau\omega) = \left(\omega^2 - m_2\right) e^{\mu_1 \tau} \\ m_3 \omega \cos(\omega\tau) - m_4 \sin(\omega\tau) = -e^{\mu_1 \tau} m_1 \omega \end{cases} \tag{4}$$

Add the squares of the two equations in equation system (4), we get,

$$\omega^4 + m_5 \omega^2 + m_6 = 0 \tag{5}$$

where

$$m_5 = m_1 - 2m_2 - m_3^2 e^{-2\mu_1 \tau}, m_6 = m_2^2 - m_4^2 e^{-2\mu_1 \tau}.$$

Theorem 1: When $\tau = \tau_0$, the Hopf bifurcation occurred near the endemic equilibrium E_* of system (**??**sec1), and generated a cluster of periodic solutions.

Let us solve the two equations of equation (4) simultaneously, the critical value of time delay can be determined:

$$\tau_l = \frac{1}{\omega} \arctan \frac{m_2 m_3 \omega - m_3 \omega^3}{m_1 m_3 \omega^2 + m_2 m_4 - m_4 \omega^2} + \frac{l\pi}{\omega}$$

where $l = 0, 1, 2 \ldots.$

According to the previous conditions, it can be inferred that equation (5) has only one true root ω_0:

$$\omega_0 = \left[\frac{\left(2m_2 + m_3^2 e^{-2\mu_1 \tau} - m_1\right) + \sqrt{\left(m_1 - 2m_2 - m_3^2 e^{-2\mu_1 \tau}\right)^2 - 4m_2^2 - m_4^2 e^{-2\mu_1 \tau}}}{2} \right]^{\frac{1}{2}}$$

Then take the derivative of equation (3) on τ,

$$\left(\frac{d\lambda}{d\tau}\right)^{-1} = \frac{m_3 \lambda \tau + m_4 \tau - m_3 - (2\lambda + m_1)\, e^{(\mu_1 + \lambda)\tau}}{(\lambda + \mu_1)(m_3 \lambda + m_4)}$$

and substitute $\lambda = i\omega$, $\tau = \tau_0$, such that

$$\begin{aligned} \mathrm{Re}\left[\left(\frac{d\lambda}{d\tau}\right)^{-1}\right] &= \mathrm{Re}\left[\frac{m_3 \lambda \tau + m_4 \tau - m_3 - (2\lambda + n_1)\, e^{(\mu_1 + \lambda)\tau}}{(\lambda + \mu_1)(m_3 \lambda + m_4)}\right] \\ &= \frac{m_3^2 \omega^2 \mu_1 \tau + m_4^2 \mu_1 \tau - m_3 m_4 \mu_1 + m_3^2 \omega^2}{(\mu_1^2 + \omega^2)(m_4^2 + m_3^2 \omega^2)} \\ &\quad - \frac{e^{\mu_1 \tau}\left[\cos(\omega\tau)\left(2m_4 \omega^2 + 2m_3 \mu_1 \omega^2 + m_1 m_4 \mu_1 - m_1 m_3 \omega^2\right)\right.}{(\mu_1^2 + \omega^2)(m_4^2 + m_3^2 \omega^2)} \\ &\quad + \frac{\left.\sin(\omega\tau)\left(m_1 m_4 \omega + m_1 m_3 \mu_1 \omega - 2\mu_1 m_4 \omega + 2m_3 \omega^3\right)\right]}{(\mu_1^2 + \omega^2)(m_4^2 + m_3^2 \omega^2)} \end{aligned} \tag{6}$$

Combine two equations of (4) to get,

$$\begin{cases} \cos(\omega\tau) = \dfrac{e^{\mu_1 \tau}\left(m_4 \omega^2 - m_2 m_4 - m_1 m_3 \omega^2\right)}{m_4^2 + m_3^2 \omega^2} \\ \sin(\omega\tau) = \dfrac{e^{\mu_1 \tau}\left(m_3 \omega^3 + m_1 m_4 \omega - m_2 m_3 \omega\right)}{m_4^2 + m_3^2 \omega^2} \end{cases} \tag{7}$$

Then, substitute equation (7) into equation (6), the transversality condition can be obtained:

$$\begin{aligned} \mathrm{Re}\left[\left(\frac{d\lambda}{d\tau}\right)^{-1}\right] &= \frac{m_3^2 \omega^2 \mu_1 \tau + m_4^2 \mu_1 \tau - m_3 m_4 \mu_1 + m_3^2 \omega^2}{(\mu_1^2 + \omega^2)(m_4^2 + m_3^2 \omega^2)} \\ &\quad - \frac{e^{2\mu_1 \tau}\left[n_1 \omega^6 + n_2 \omega^4 + n_3 \omega^2 + n_4 \omega - n_5\right]}{(\mu_1^2 + \omega^2)\left(m_4^2 + m_3^2 \omega^2\right)^2} \end{aligned}$$

where

$$n_1 = 2m_3^2, n_2 = 2m_4^2 + m_1^2 m_3^2 - m_1 m_3^2 \mu_1 - 2m_2 m_3^2,$$
$$n_3 = m_1^2 m_4^2 - 2m_2 m_4^2 - m_1^2 m_3 m_4 \mu_1 - m_1 m_2 m_3^2 \mu_1 - m_1 m_4^2 \mu_1,$$
$$n_4 = m_1^2 m_3 m_4 \mu_1, n_5 = -m_1 m_2 m_4^2 \mu_1.$$

When $\mathcal{R}_0 < 1$ and $\omega_0 > 0$, we can obtain Re $\left[\left(\frac{d\lambda}{d\tau}\right)^{-1}\right] > 0$.

H_1 When $\tau = \tau_0$, the characteristic equation has a pair of simple pure imaginary roots $\pm i\omega$. According to the implicit function theorem, for τ that is sufficiently close to τ_0, the corresponding eigenvalue can be formulated as $\omega(\tau)i + \alpha(\tau) = \lambda(\tau)$, and $\omega(\tau_0) = \omega_0$, $\alpha(\tau_0) = 0$. It can be concluded that as τ increases and passes through τ_0, the above characteristic roots cross the imaginary axis.

H_2 The transverse condition Re $\left[\left(\frac{d\lambda}{d\tau}\right)^{-1}\right] > 0$.

H_3 When $\tau = \tau_0$, equation (3) possesses negative real parts for all roots except for $\pm i\omega_0$; when $\tau \in [0, \tau_0)$, all roots hold a negative real part; when $\tau \in (\tau_l, \tau_{l+1}]$, there are $2(l+1)$ roots with positive real parts.

Then $G(0) = \beta\gamma e^{-\mu_1\tau} + 2\mu + \xi - 2\mu(\mu + \xi) < 0$, and when $\lambda \to +\infty, G(\lambda) \to +\infty$.

With H_1–H_3, we can obtain when $\tau = \tau_0$, there is at least one root that displays a positive real component and traverses the imaginary axis from left to right. That is to say, as $\tau = \tau_0$, there is the Hopf bifurcation near E_*. The proof is completed.

2.2.3 The direction of bifurcation and the periodic solutions

We will employ the centre manifold theorem (Carr, 2012) along with the normal form method (Kuznetsov et al., 1998) in our analysis. By combining these two approaches, we can gain deeper insights into the system's dynamics.

Due to μ_1 being small enough, $e^{-\mu_1\tau} \to 1$.

In addition to the definitions already provided in the previous text, the variables and notations of this section are shown in Table 2.

Table 2 The variables and notations of Section 2.2.3

D	A feasible domain
y, j, x, u	The function defined in the feasible domain
$L, \phi, \kappa, \varphi, A, R, M, N$	The operator defined within the feasible domain
$\varrho_1, \varrho_2, \theta, \vartheta, \epsilon, h$	The variable defined in the feasible domain
χ	Dirac function
$\overline{M}$	The conjugate operator of M
A^*	The adjoint operator of A
q, q_1	The characteristic vector

Assume $\varrho_1 = S - S^*$, $\varrho_2 = I - I^*$, $\tau = \tau_0 + \vartheta$, we translate system (2) into the equation defined in $D = D([-1, 0], \mathbf{R}^2)$,

$$\dot{y}(t) = L_\vartheta(y_t) + j(\vartheta, y_t) \tag{8}$$

where $y_t(\theta) = y(t+\theta), L_\vartheta : \mathbf{C} \to \mathbf{R}^2, j : \mathbf{R} \times \mathbf{C} \to \mathbf{R}^2$, i.e.,

$$L_\vartheta \phi = (\tau_0 + \vartheta) \begin{pmatrix} -\frac{\beta\gamma}{\mu+\xi} - \mu & 0 \\ \frac{\beta\gamma}{\mu+\xi} & -(\mu+\xi) \end{pmatrix} \begin{pmatrix} \phi_1(0) \\ \phi_2(0) \end{pmatrix} + (\tau_0 + \vartheta) \begin{pmatrix} 0 & -(\mu+\xi) \\ 0 & \mu+\xi \end{pmatrix} \begin{pmatrix} \phi_1(-1) \\ \phi_2(-1) \end{pmatrix}$$

and $j(\vartheta, y_t) = (\tau_0 + \vartheta) \begin{pmatrix} -\beta\phi_1(0)\phi_2(-1) \\ \beta\phi_1(0)\phi_2(-1) \end{pmatrix}$.

Due to Riesz representation theorem (Goodrich, 1970), for $\epsilon \in [-1, 0]$, there exists $\kappa(\epsilon, \vartheta)$ such that

$$L_\vartheta(\phi) = \int_{-1}^{0} d\kappa(\epsilon, \vartheta)\phi(\epsilon)$$

where $\phi \in \mathbf{C}([-1, 0], \mathbf{R}^2)$.

Then, we can construct

$$\kappa(\epsilon, \vartheta) = (\tau_0 + \vartheta) \begin{pmatrix} -\frac{\beta\gamma}{\mu+\xi} - \mu & 0 \\ \frac{\beta\gamma}{\mu+\xi} & -(\mu+\xi) \end{pmatrix} \chi(\epsilon) - (\tau_0 + \vartheta) \begin{pmatrix} 0 & -(\mu+\xi) \\ 0 & \mu+\xi \end{pmatrix} \chi(\epsilon+1)$$

where χ is Dirac function.

The definition is as follows:

$$A(\vartheta)\phi = \begin{cases} \frac{d\phi(\epsilon)}{d\epsilon}, & \epsilon \in [-1, 0), \\ \int_{-1}^{0} d\kappa(s, \vartheta)\phi(s), & \epsilon = 0. \end{cases}$$

$$R(\vartheta)\phi = \begin{cases} 0, & \epsilon \in [-1, 0), \\ j(\vartheta, \phi), & \epsilon = 0. \end{cases}$$

Equation (8) can be converted to:

$$\dot{y}(t) = A(\vartheta)y_t + y_t R(\vartheta) \tag{9}$$

Define the adjoint operator $A^*(0)$ as:

$$A^*(0)\varphi(s) = \begin{cases} -\frac{d\psi(h)}{dh}, & h \in (0, 1], \\ \int_{-1}^{0} d\kappa(t, 0)\varphi(-t), & h = 0 \end{cases} \tag{10}$$

Subsequently, bilinear inner product is formulated as:

$$\langle \varphi, \phi \rangle = \overline{\varphi}(0)\varphi(0) - \int_{\epsilon=-1}^{0} \int_{\varsigma=0}^{\epsilon} \overline{\varphi}^T(\varsigma - \epsilon) d\kappa(\epsilon)\phi(\varsigma) d\varsigma \tag{11}$$

Here is conjugate operator $A^* = A^*(0)$ and $A = A(0)$.

From the previous discussion, $\pm i\omega_0\tau_0$ is the characteristic root of both A and A^*, so we should calculate A and A^* are respectively related to the eigenvectors of eigenvalues $i\omega_0\tau_0$ and $-i\omega_0\tau_0$.

Assume A_0 is the eigenvector of characteristic value $i\omega_0\tau_0$, such that, $A_0 q(\epsilon) = i\omega_0\tau_0 q(\epsilon)$, $q(\epsilon) = (1, q_1(0))^T e^{i\omega_0\tau_0\epsilon}$.

Especially, when $\epsilon = 0$ also holds true, as follow:

$$\kappa(0,0)q(0) - \kappa(-1,0)q(-1) = i\omega_0\tau_0 q(0)$$

By substituting and organising, we can obtain,

$$\begin{aligned} &\tau_0 \begin{pmatrix} -\frac{\beta\gamma}{\mu+\xi} - \mu & 0 \\ \frac{\beta\gamma}{\mu+\xi} & -(\mu+\xi) \end{pmatrix} \begin{pmatrix} 1 \\ q_1 \end{pmatrix} - \tau_0 e^{-i\omega_0\tau_0} \begin{pmatrix} 0 & -(\mu+\xi) \\ 0 & \mu+\xi \end{pmatrix} \begin{pmatrix} 1 \\ q_1 \end{pmatrix} \\ &= i\omega_0\tau_0 \begin{pmatrix} 1 \\ q_1 \end{pmatrix} \end{aligned}$$

At this time, the solution of the above equation $q_1 = -\frac{\mu+i\omega_0}{i\omega_0+\mu+\xi}$.

Similarly, assume $q^*(h) = M(1, q_1^*(h))e^{i\omega_0\tau_0 h}$ is A_0^* is the eigenvector of characteristic value $-i\omega_0\tau_0$, such that, $A_0^* q^*(h) = -i\omega_0\tau_0 q^*(h)$.

Particularly, when $h = 0$, combine equation (10), as follows:

$$A^*(0)q^*(0) = -q^*(1)\kappa(-1,0) + q^*(0)\kappa(0,0)$$

Then, substitute and obtain,

$$\begin{aligned} &M\left(1, q_1^*(h)\right)\tau_0 \begin{pmatrix} -\frac{\beta\gamma}{\mu+\xi} - \mu & 0 \\ \frac{\beta\gamma}{\mu+\xi} & -(\mu+\xi) \end{pmatrix} - e^{i\omega_0\tau_0} M\left(1, q_1^*(h)\right)\tau_0 \begin{pmatrix} 0 & -(\mu+\xi) \\ 0 & \mu+\xi \end{pmatrix} \\ &= -i\omega_0\tau_0 M\left(1, q_1^*(h)\right) \end{aligned}$$

The solution of the above equation is $q_1^* = \frac{(\mu-i\omega_0)(\mu+\xi)}{\beta\gamma} + 1$.

To make $\langle q^*(h), q(\epsilon)\rangle = 1$, it is necessary to find M according to equation (11),

$$\begin{aligned} \langle q^*(h), q(\epsilon)\rangle &= \overline{M}\left(1, \overline{q}_1^*\right)\left(1, q_1\right)^T \\ &\quad - \int_{-1}^{0}\int_{\varsigma=0}^{\epsilon} \overline{M}\left(1, \overline{q}_1^*\right) e^{-i\omega_0\tau_0(\varsigma-\epsilon)} d\kappa(\epsilon)\left(1, q_1\right)^T e^{i\omega_0\tau_0\varsigma} d\varsigma \\ &= \overline{M}\left[1 + \overline{q}_1^* q_1 + \tau_0(\mu+\xi)\left(q_1\overline{q}_1^* - q_1\right)e^{-i\omega_0\tau_0}\right] \end{aligned}$$

We can get

$$\begin{aligned} \overline{M} &= \frac{1}{1 + \overline{q}_1^* q_1 + \tau_0(\mu+\xi)(q_1\overline{q}_1^* - q_1)e^{-i\omega\tau_0}}, \\ M &= \frac{1}{1 + q_1^*\overline{q}_1 + \tau_0(\mu+\xi)(\overline{q}_1 q_1^* - \overline{q}_1)e^{i\omega\tau_0}}. \end{aligned}$$

Then we compute the parameters of the central manifold at $\vartheta = 0$.

Firstly, define

$$x(t) = \langle q^*, y_t \rangle \, , N(t,\epsilon) = y_t - 2\,\mathrm{Re}\,\{x(t)q(\epsilon)\} = N(x(t), \overline{x}(t), \epsilon)$$

where

$$N(x(t), \overline{x}(t), \epsilon) = \frac{N_{20}(\epsilon)}{2} x^2 + N_{11}(\epsilon) x\overline{x} + \frac{N_{02}(\epsilon)}{2} \overline{x}^2 + \cdots \tag{12}$$

Here, x and $\overline{x}$ serve as the local coordinates that correspond to the centre manifold in the q^* and $\overline{q}^*$ directions, respectively.

$$\begin{aligned}
\dot{x}(t) &= \langle q^*, \dot{u}(t) \rangle = \langle q^*, Au_t + Ru_t \rangle = \langle q^*, Au_t \rangle + \langle q^*, Ru_t \rangle \\
&= i\omega_0\tau_0 z + \overline{q}^*(0) f(0, N(x, \overline{x}, 0) + 2\,\mathrm{Re}\,\{xq(\epsilon)\}) \\
&= i\omega_0\tau_0 x + \overline{q}^*(0) f_0(x, \overline{x}) = i\omega_0\tau_0 x + p(x, \overline{x})
\end{aligned}$$

where

$$p(x, \overline{x}) = \frac{p_{20}}{2} x^2 + p_{11} x\overline{x} + \frac{p_{02}}{2} \overline{x}^2 + \frac{p_{21}}{2} x^2\overline{x} + \cdots \tag{13}$$

Considering the define of $j(\vartheta, y_t)$,

$$p(x, \overline{x}) = q^*(0) j_0(x, \overline{x}) = \overline{M}(1, \overline{q}_1^*)\tau_0 \begin{pmatrix} -\beta y_{1t}(0) y_{2t}(-1) \\ \beta y_{1t}(0) y_{2t}(-1) \end{pmatrix}$$

Due to $y_t(0) = 2\,\mathrm{Re}\,\{x(t)q(0)\} + N(t, 0)$, i.e.,

$$\begin{aligned}
y_{1t}(0) &= N(t, 0) + 2\,\mathrm{Re}\,\{x(t)q(0)\} = N^{(1)}(x(t), \overline{x}(t), 0) + x(t) + \overline{x}(t) \\
&= \frac{N_{20}^{(1)}(0)}{2} x^2 + N_{11}^{(1)}(0) x\overline{x} + x + \overline{x} + \frac{N_{02}^{(1)}(0)}{2} \overline{x}^2 + o(|(x, \overline{x})|^3)
\end{aligned}$$

Likewise,

$$\begin{aligned}
y_{1t}(-1) &= N(t, -1) + 2\,\mathrm{Re}\,\{x(t)q(-1)\}\, , \\
y_{2t}(-1) &= N^{(2)}(x(t), \overline{x}(t), -1) + 2\,\mathrm{Re}\,\left\{x(t) q_1 e^{-i\omega_0\tau_0}\right\} \\
&= \frac{N_{20}^{(2)}(-1)}{2} x^2 + N_{11}^{(2)}(-1) x\overline{x} + \frac{N_{02}^{(2)}(-1)}{2} \overline{x}^2 \\
&\quad + x(t) q_1 e^{-i\omega_0\tau_0} + o(|(x, \overline{x})|^3).
\end{aligned}$$

Then compare coefficients, obtain:

$$\begin{aligned}
p_{20} &= 2\overline{M}\tau_0(\overline{q_1}^* - 1)\beta q_1 e^{-i\omega_0\tau_0}, \\
p_{11} &= 2\overline{M}\tau_0(\overline{q_1}^* - 1)\beta\,\mathrm{Re}\,\left\{q_1 e^{-i\omega_0\tau_0}\right\}, \\
p_{02} &= 2\overline{M}\tau_0(\overline{q_1}^* - 1)\beta q_1 e^{i\omega_0\tau_0}, \\
p_{21} &= 2\overline{M}\tau_0\beta \Bigg[(\overline{q_1}^* - 1) \Bigg(\frac{1}{2}\overline{q}_1 e^{i\omega_0\tau_0} N_{20}^{(1)}(0) + N_{11}^{(1)}(0) q_1 e^{-i\omega_0\tau_0} \\
&\qquad + N_{11}^{(2)}(-1) + \frac{N_{20}^{(2)}(-1)}{2} \Bigg) \Bigg].
\end{aligned}$$

Due to $\dot{N} = \dot{y}_t - \dot{x} \cdot q - \dot{\overline{x}} \cdot \overline{q}$,

$$\begin{aligned} \dot{N} &= \begin{cases} AN - 2\operatorname{Re}\{\overline{q}^*(0) f_0 q(\epsilon)\}, & \epsilon \in [-1, 0) \\ AN - 2\operatorname{Re}\{\overline{q}^*(0) f_0 q(\epsilon)\} + j_0, & \epsilon = 0 \end{cases} \\ &= AN + B(x, \overline{x}, \epsilon) \end{aligned} \tag{14}$$

where

$$B(x(t), \overline{x}(t), \epsilon) = \frac{B_{20}(\epsilon)}{2} x^2 + B_{11}(\epsilon) x\overline{x} + \frac{B_{02}(\epsilon)}{2} \overline{x}^2 + \cdots \tag{15}$$

Combine (12) and (14),

$$\begin{aligned} \dot{N} &= N_{20} x\dot{x} + N_{11} \dot{x}\overline{x} + N_{11} x\dot{\overline{x}} + \cdots \\ &= N_{20} i\omega_0\tau_0 x^2 + \frac{N_{20} p_{20}}{2} x^3 + N_{20} p_{11} x^2 \overline{x} + \frac{N_{20} p_{02}}{2} x\overline{x}^2 \\ &+ \frac{N_{20} p_{21}}{2} x^3 \overline{x} + \cdots \end{aligned} \tag{16}$$

Due to $AN = \frac{AN_{20}(\epsilon)}{2} x^2 + AN_{11}(\epsilon) x\overline{x} + \frac{AN_{02}(\epsilon)}{2} \overline{x}^2 + \cdots$, we get,

$$\begin{aligned} AN + B = {} & \frac{B_{20}(\epsilon)}{2} x^2 + \frac{AN_{20}(\epsilon)}{2} x^2 + [AN_{11}(\epsilon) + B_{11}(\epsilon)] x\overline{x} \\ & + \frac{AN_{02}(\epsilon) + B_{02}(\epsilon)}{2} \overline{x}^2. \end{aligned} \tag{17}$$

Then comparing (16) and (17), we can obtain,

$$N_{11}(\epsilon) A = -B_{11}(\epsilon), (2i\omega_0\tau_0 - A) N_{20}(\epsilon) = B_{20}(\epsilon). \tag{18}$$

According to (14), we analyse when $\epsilon \in [-1, 0)$,

$$\begin{aligned} B(x, \overline{x}, \epsilon) &= -2\operatorname{Re}\{\overline{q}^*(0) j_0 q(\epsilon)\} \\ &= -\frac{1}{2} [p_{20} q(\epsilon) + \overline{p}_{02} \overline{q}(\epsilon)] x^2 - [p_{11} q(\epsilon) + \overline{p}_{11} \overline{q}(\epsilon)] x\overline{x} + \cdots \end{aligned}$$

Base on the coefficients of equation (15),

$$B_{11}(\epsilon) = -q(\epsilon) p_{11} - \overline{p}_{11} \overline{q}(\epsilon), B_{20}(\epsilon) = -p_{20} q(\epsilon) - \overline{p}_{02} \overline{q}(\epsilon). \tag{19}$$

Combine (18), (19) and A,

$$\dot{N}_{20}(\epsilon) = \overline{q}(\epsilon) \overline{p}_{02} + 2i\omega_0\tau_0 N_{20}(\epsilon) + p_{20} q(\epsilon). \tag{20}$$

Solving equation (20),

$$N_{20}(\epsilon) = \frac{i p_{20}}{\omega_0\tau_0} q(0) e^{i\omega_0\tau_0\epsilon} + \frac{i\overline{p}_{02}}{3\omega_0\tau_0} \overline{q}(0) e^{-i\omega_0\tau_0\epsilon} + C_1 e^{2i\omega_0\tau_0\epsilon},$$

where $C_1 = (C_{11}, C_{12})^T \in \mathbf{R}^2$.

Similarly, we can obtain:

$$\dot{N}_{11}(\epsilon) = \overline{p}_{11}\overline{q}(\epsilon) + q(\epsilon)p_{11}. \tag{21}$$

Solve equation (21),

$$N_{11}(\theta) = -\frac{ig_{11}}{\omega_0\tau_0}q(0)e^{i\omega_0\tau_0\epsilon} + \frac{i\overline{p}_{11}}{\omega_0\tau_0}\overline{q}(0)e^{-i\omega_0\tau_0\epsilon} + C_2,$$

where $C_2 = (C_{21}, C_{22})^T \in \mathbf{R}^2$.

Then, we need to determine the values of C_1 and C_2. According to equation (18) and A, we can obtain,

$$\begin{aligned}\int_{-1}^{0} d\kappa(\epsilon)N_{20}(\epsilon) &= -B_{20}(\epsilon) + 2i\omega_0\tau_0 N_{20}(\epsilon),\\ \int_{-1}^{0} d\kappa(\epsilon)N_{11}(\epsilon) &= -B_{11}(\epsilon).\end{aligned} \tag{22}$$

According to $q(\epsilon)$ is the eigenvector of $A(0)$,

$$\begin{aligned}\int_{-1}^{0} d\epsilon(\epsilon)N_{20}(\epsilon) &= \frac{ip_{20}}{\omega_0\tau_0}\int_{-1}^{0} d\kappa(\epsilon)q(\epsilon) + \frac{i\overline{p}_{02}}{3\omega_0\tau_0}\int_{-1}^{0} d\kappa(\epsilon)\overline{q}(\epsilon)\\ &\quad + \int_{-1}^{0} d\kappa(\epsilon)C_1 e^{2i\omega_0\tau_0\epsilon}\\ &= \int_{-1}^{0} d\kappa(\epsilon)C_1 e^{2i\omega_0\tau_0\epsilon} - p_{20}q(0) + \frac{\overline{p}_{02}}{3}\overline{q}(0).\end{aligned}$$

Due to $2i\omega_0\tau_0 N_{20}(0) = -2p_{20}q(0) - \frac{2\overline{p}_{02}}{3}\overline{q}(0) + 2i\omega_0\tau_0 C_1$, the two equations of equation (22) become:

$$B_{20}(0) = -p_{20}q(0)\overline{q}(0) + \left[2i\omega_0\tau_0 - \int_{-1}^{0} d\kappa(\epsilon)e^{2i\omega_0\tau_0\epsilon}\right]C_1 - \overline{p}_{02}, \tag{23}$$

$$B_{11}(0) = -\overline{p}_{11}\overline{q}(0) - \int_{-1}^{0} d\kappa(\epsilon)C_2 - p_{11}q(0). \tag{24}$$

Base on the equation (14),

$$\begin{aligned}B(x,\overline{x},0) &= -2\,\mathrm{Re}\,\{\overline{q}^*(0)j_0q(0)\} + j_0(x,\overline{x})\\ &= -\frac{1}{2}\left[\overline{q}(0)\overline{p}_{02} + p_{20}q(0)\right]x^2 - \overline{x}x\left[\overline{q}(0)\overline{p}_{11} + p_{11}q(0)\right]\\ &\quad + \cdots + j_0(x,\overline{x}).\end{aligned} \tag{25}$$

Then, from equation (15), we can obtain,

$$B(x(t),\overline{x}(t),0) = \frac{B_{20}(0)}{2}x^2 + B_{11}(0)x\overline{x} + \frac{B_{02}(0)}{2}\overline{x}^2 + \cdots \tag{26}$$

Subsequently, due to

$$
\begin{aligned}
j_0(x,\overline{x}) &= \tau_0 \begin{pmatrix} -\beta y_{1t}(0)y_{2t}(-1) \\ \beta y_{1t}(0)y_{2t}(-1) \end{pmatrix} \\
&= \tau_0 \begin{pmatrix} -\beta q_1 e^{-i\omega_0\tau_0} \\ \beta q_1 e^{-i\omega_0\tau_0} \end{pmatrix} x^2 + \tau_0 \begin{Bmatrix} -2\beta\,\mathrm{Re}\left\{q_1 e^{-i\omega_0\tau_0}\right\} \\ 2\beta\,\mathrm{Re}\left\{q_1 e^{-i\omega_0\tau_0}\right\} \end{Bmatrix} x\overline{x} + \cdots
\end{aligned}
\tag{27}
$$

Hence, according to (25), (26) and (27),

$$
B_{20}(0) = -\overline{q}(0)\overline{p}_{02} + (-\beta\tau_0 q_1 e^{-i\omega_0\tau_0}, \beta\tau_0 q_1 e^{-i\omega_0\tau_0})^T - q(0)p_{20}, \tag{28}
$$

$$
\begin{aligned}
B_{11}(0) &= (-2\beta\tau_0\,\mathrm{Re}\left\{q_1 e^{-i\omega_0\tau_0}\right\}, 2\beta\tau_0\,\mathrm{Re}\left\{q_1 e^{-i\omega_0\tau_0}\right\})^T \\
&\quad - \overline{q}(0)\overline{p}_{11} - p_{11}q(0).
\end{aligned}
\tag{29}
$$

Comparing (23) and (28), we can obtain:

$$
C_1 = 2 \begin{pmatrix} 2i\omega_0 + \frac{\beta\gamma}{\mu+\xi} + \mu & (\mu+\xi)e^{-2i\omega_0\tau_0} \\ -\frac{\beta\gamma}{\mu+\xi} & 2i\omega_0 + (\mu+\xi)(1-e^{-2i\omega_0\tau_0}) \end{pmatrix}^{-1} \begin{pmatrix} -\beta\tau_0 q_1 e^{-i\omega_0\tau_0} \\ \beta\tau_0 q_1 e^{-i\omega_0\tau_0} \end{pmatrix}.
$$

Similarly, we can obtain,

$$
C_2 = 2 \begin{pmatrix} \frac{\beta\gamma}{\mu+\xi} + \mu & \mu+\xi \\ -\frac{\beta\gamma}{\mu+\xi} & 0 \end{pmatrix}^{-1} \begin{pmatrix} -\beta\tau_0\,\mathrm{Re}\left\{q_1 e^{-i\omega_0\tau_0}\right\} \\ \beta\tau_0\,\mathrm{Re}\left\{q_1 e^{-i\omega_0\tau_0}\right\} \end{pmatrix}.
$$

Then we substitute and obtain the value of p_{21}, $N_{11}(\epsilon)$ and $N_{20}(\epsilon)$. Ultimately, we also proceed to compute the subsequent values:

$$
\begin{aligned}
V &= \frac{ip_{11}p_{20}}{2\omega_0\tau_0} + \frac{p_{21}}{2} - \frac{i\left|p_{11}\right|^2}{\omega_0\tau_0} - \frac{\left|p_{02}\right|^2 i}{6\omega_0\tau_0}, \\
X &= -\frac{\mathrm{Re}\left\{V\right\}}{\mathrm{Re}\left\{y'(\tau_0)\right\}}, \\
Y &= 2\,\mathrm{Re}\left\{V\right\}, \\
Z &= -\frac{\mathrm{Im}\left\{V\right\} + \upsilon\,\mathrm{Im}\left\{y'(\tau_0)\right\}}{\omega_0\tau_0}.
\end{aligned}
$$

Based on the inherent attributes of bifurcation periodic solutions, the subsequent theorem can be logically deduced.

Theorem 2:

1. When $X < 0$ ($X > 0$), the system generates a subcritical (supercritical) Hopf bifurcation.
2. When $Y < 0$ ($Y > 0$), the periodic solution is stable (unstable).
3. When $Z < 0$ ($Z > 0$), the period of a bifurcation periodic solution undergoes a decrease (increase) as the value of τ is incremented.

3 Numerical simulation

In this research paper, we formulate a delayed SIR system pertaining to the dynamics of infectious diseases. We take different values for the parameters of the DDE system and conduct numerical simulations using MATLAB to verify its reliability and authenticity.

To exemplify the behaviour of system (2), we present two numerical examples. The numerical simulation is carried out with fixed parameters $\mu_1 = 0.002$, $\gamma = 0.5$, $\mu = 0.2$, $\xi = 0.3$, $\beta = 0.007$. These data are derived from the actual biological significance discussed in the previous article (Constantino et al., 2025) and are more suitable for fitting this model. Based on the theoretical knowledge in the article, we can calculate the critical value $\tau_0 = 0.85$.

1 Firstly, we set $\tau = 0.5 < \tau_0$. Next, we provide initial values $S(0) = 2$, $I(0) = 1$. Time series figures of various variables S and R at E_* when $\tau < \tau_0$ is presented in Figures 2 and 3.

Figure 2 When $\tau < \tau_0$, the time series figure of S (see online version for colours)

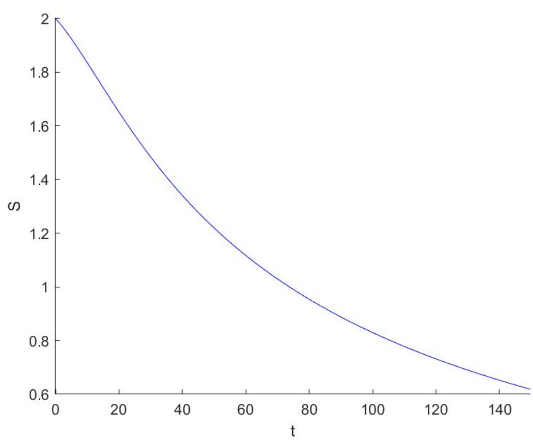

Figure 3 When $\tau < \tau_0$, the time series figure of I (see online version for colours)

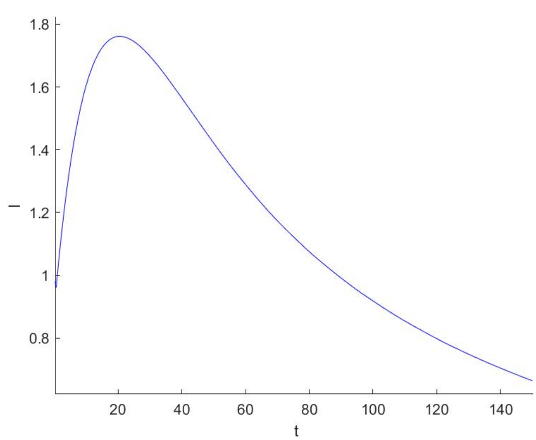

From Figures 2–3, we can know when $\tau < \tau_0$, the equilibrium E_* is determined to be globally stable. It can be seen that both susceptible (S) and infected individuals (I) eventually tend to stabilise, indicating that the disease has been controlled.

2 Subsequently, we set $\tau = 1.2 > \tau_0$. The initial value is the same as no. 1, it suggests that E_* is unstable and exhibits oscillatory behaviour (see Figures 4 and 5). As shown in the Figures 4 and 5, the equilibrium point is in an unstable state. When τ exceed the delay threshold τ_0, the disease may be more likely to spiral out of control, leading to large-scale outbreaks.

Figure 4 When $\tau > \tau_0$, the time series figure of S (see online version for colours)

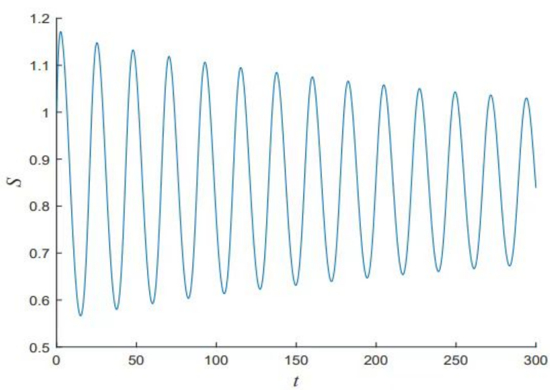

Figure 5 When $\tau > \tau_0$, the time series figure of I (see online version for colours)

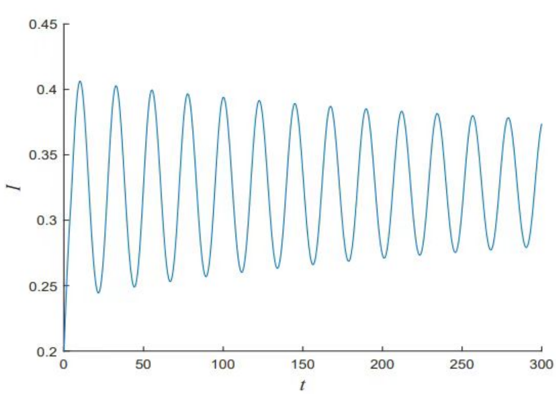

From Figure 6, we can see that the equilibrium point is unstable, resulting in Hopf bifurcation which reveals the stability transition of the epidemic model under the change of specific parameters, such as the transition from stable state to periodic oscillation.

Figure 6 Trajectory diagram of S changing with I (see online version for colours)

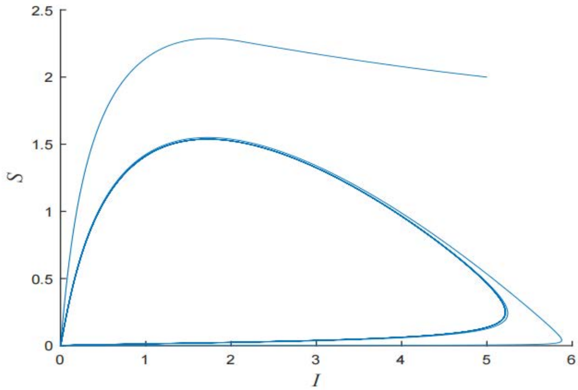

4 Conclusions

Firstly, through a detailed analysis of the local stability of the equilibrium point in the model, we have determined the delay threshold τ_0 for triggering Hopf bifurcation. When the time delay exceeds this threshold, the system will transition from a stable state to an oscillatory state, characterised by the appearance of periodic solutions. Subsequently, we utilised the central manifold theorem and normal form theory as our analytical tools to delve into the direction of bifurcations and periodic solutions. Furthermore, we conducted numerical simulations using MATLAB to verify the reliability and authenticity of our theoretical analysis. By setting different values for the parameters of the delayed differential equation (DDE) system and observing the resulting time series figures, we were able to visualise the system's behaviour and confirm our findings. Specifically, when the time delay was below the threshold ($\tau < \tau_0$), the equilibrium point was stable, with both susceptible and infected individuals eventually tending towards the equilibrium values. However, when the time delay exceeded the threshold ($\tau > \tau_0$), the equilibrium point became unstable and exhibited oscillatory behaviour, consistent with our theoretical predictions.

It is found that the significant impact of time delay on the dissemination of infectious diseases. Through the formulation of a delayed SIR model and the application of thorough mathematical analysis, we have gained profound insights into the system's behaviour and how it is influenced by delays. Our key findings indicate that delays can trigger system instability, the appearance of periodic solutions, and bifurcations, all of which hold significant ramifications for the prevention and control of infectious diseases. Furthermore, our research underscores the importance of controlling the disease before reaching a critical threshold of time delay. By comprehending these intricate dynamics, we can enhance our predictive capabilities regarding the behaviour of infectious diseases and devise more potent strategies for their management and mitigation.

In summary, our research not only suggests effective prevention and control measures but also significantly contributes to the theoretical understanding of time-delay models in the context of infectious diseases. Our contributions enrich the existing knowledge of time-delay models in infectious disease dynamics and further advance the theoretical framework of such models. By providing a deeper understanding of how delays influence the dissemination of infectious diseases, our work paves the way for the development of more accurate and effective disease management strategies, ultimately enhancing our ability to combat and mitigate the impact of infectious diseases on public health.

References

Barman, M. and Mishra, N. (2023) 'Hopf bifurcation in a networked delay SIR epidemic model', *Journal of Mathematical Analysis and Applications*, Vol. 525, No. 1, p.127131.

Carr, J. (2012) *Applications of Centre Manifold Theory*, Vol. 35, Springer Science & Business Media, Berlin.

Constantino, C., Luísa, M., Pedro, L., Niel, H. and Baltazar, N. (2025) 'A fractional order SIR model describing hesitancy to the COVID-19 vaccination', *Applied Numerical Mathematics*, Vol. 207, No. 3, pp.608–620.

Cui, A.J., Ma, Y.H., Li, C. and Wang, X.M. (2022) 'Retrieval method for multi-level network malicious intrusion information based on sequential logic model', *International Journal of Information and Communication Technology*, Vol. 21, No. 4, pp.386–397.

Damgacioglu, H., Lin, Y.Y., Ortiz, A.P., Wu, C.F., Shahmoradi, Z., Shyu, S.S., Li, R., Nyitray, A.G., Sigel, K., Clifford, G.M. and Jay, N. (2023) 'State variation in squamous cell carcinoma of the anus incidence and mortality, and association with HIV/AIDS and smoking in the United States', *Journal of Clinical Oncology*, Vol. 41, No. 6, pp.1228–1238.

DeWitte, S.N. (2018) 'Stress, sex, and plague: patterns of developmental stress and survival in pre- and post-Black Death London', *American Journal of Human Biology*, Vol. 30, No. 1, p.e23073.

Goodrich, R.K. (1970) 'A Riesz representation theorem', *Proceedings of the American Mathematical Society*, Vol. 24, No. 3, pp.629–636.

Kermack, W.O. and McKendrick, A.G. (1927) 'A contribution to the mathematical theory of epidemics', *Proceedings of the Royal Society of London. Series A, Containing Papers of a Mathematical and Physical Character*, Vol. 115, No. 772, pp.700–721.

Kuznetsov, Y.A., Kuznetsov, I.A. and Kuznetsov, Y. (1998) *Elements of Applied Bifurcation Theory*, Vol. 112, Springer, Berlin.

Leowski, C. (2010) 'Multidimensional vector coordinates as a method of organisation of large social and economic databases', *International Journal of Information and Communication Technology*, Vol. 2, No. 4, pp.374–385.

Lestari, D. (2016) 'Local stability of AIDS epidemic model through treatment and vertical transmission with time delay', *Journal of Physics: Conference Series*, Vol. 693, No. 1, p.012010.

Li, T., Zhang, F., Liu, H. and Chen, Y. (2017) 'Threshold dynamics of an SIRS model with nonlinear incidence rate and transfer from infectious to susceptible', *Applied Mathematics Letters*, Vol. 70, No. 9, pp.52–57.

Maier, G., Doan, B., O'Connor, A.M. (2021) 'The role of environmental factors in the epidemiology of infectious bovine keratoconjunctivitis', *Veterinary Clinics: Food Animal Practice*, Vol. 37, No. 2, pp.309–320.

Malik, S., Kishore, S., Nag, S., Dhasmana, A., Preetam, S., Mitra, O., León-Figueroa, D.A., Mohanty, A., Chattu, V.K., Assefi, M. and Padhi, B.K. (2023) 'Ebola virus disease vaccines: development, current perspectives & challenges', *Vaccines*, Vol. 11, No. 2, p.268.

Meng, X., Zhao, S., Feng, T. and Zhang, T. (2016) 'Dynamics of a novel nonlinear stochastic SIS epidemic model with double epidemic hypothesis', *Journal of Mathematical Analysis and Applications*, Vol. 433, No. 1, pp.227–242.

Moreira, M.A.M., Bonvicino, C.R., Soares, M.A. and Seuanez, H.N. (2010) 'Genetic diversity of neotropical primates: phylogeny, population genetics, and animal models for infectious diseases', *Cytogenetic and Genome Research*, Vol. 128, Nos. 1–3, pp.88–98.

Mvogo, A., Tiomela, S.A., Macías-Díaz, J.E. and Bertrand, B. (2023) 'Dynamics of a cross-superdiffusive sirs model with delay effects in transmission and treatment', *Nonlinear Dynamics*, Vol. 111, No. 14, pp.13619–13639.

Paton, N.I., Cousins, C., Suresh, C., Burhan, E., Chew, K.L., Dalay, V.B., Lu, Q., Kusmiati, T., Balanag, V.M., Lee, S.L. and Ruslami, R. (2008) 'Treatment strategy for rifampin-susceptible tuberculosis', *New England Journal of Medicine*, Vol. 38, No. 10, pp.873–887.

Shao, P. and Shateyi, S. (2021) 'Stability analysis of SEIRS epidemic model with nonlinear incidence rate function', *Mathematics*, Vol. 9, No. 21, p.2644.

Shoaib, M., Anwar, N., Ahmad, I., Naz, S., Kiani, A.K. and Raja, M.A.Z. (2023) 'Neuro-computational intelligence for numerical treatment of multiple delays SEIR model of worms propagation in wireless sensor networks', *Biomedical Signal Processing and Control*, Vol. 84, No. 6, p.104797.

Tchuenche, J.M. and Nwagwo, A. (2009) 'Local stability of an SIR epidemic model and effect of time delay', *Mathematical Methods in the Applied Sciences*, Vol. 32, No. 16, pp.2160–2175.

Yang, B. (2016) 'Stochastic dynamics of an SEIS epidemic model', *Advances in Difference Equations*, Vol. 2016, No. 1, p.226.

Yin, C., Li, J., Qiu, P., Yang, Z., Yang, L., Su, M. and Zhao, N. (2024) 'Research and development of community's opinion discovery and influence analysis system in social network', *International Journal of Information and Communication Technology*, Vol. 25, No. 3, pp.281–302.

Zhao, H., Lin, Y. and Dai, Y. (2014) 'An SIRS epidemic model incorporating media coverage with time delay', *Computational and Mathematical Methods in Medicine*, Vol. 2014, No. 1, p.680743.

Zhen, J., Ma, Z. and Han, M. (2006) 'Global stability of an SIRS epidemic model with delays', *Acta Mathematica Scientia*, Vol. 26, No. 2, pp.291–306.